International Journal of Scientific Engineering and Applied Science (IJSEAS) - Volume-1, Issue-4, June 2015
ISSN: 2395-3470
www.ijseas.com

Impact of the Time Interval in the Numerical Solution of Incompressible Flows

Alireza Baheri[1], Ahmad Navaserarab [2]

[1] Department of Mechanical Engineering, Islamic Azad University, Dezful Branch, Dezful , Iran
[2] Department of Mechanical Engineering, Islamic Azad University, Dezful Branch, Dezful , Iran

Abstract

In paper, we will deal with incompressible Couette flow, which represents an exact analytical solution of the Navier-Stokes equations. Couette flow is perhaps the simplest of all viscous flows, while at the same time retaining much of the same physical characteristics of a more complicated boundary-layer flow. The numerical technique that we will employ for the solution of the Couette flow is the Crank-Nicolson implicit method. Parabolic partial differential equations lend themselves to a marching solution; in addition, the use of an implicit technique allows a much larger marching step size than would be the case for an explicit solution. Hence, in the present paper we will have the opportunity to explore some aspects of CFD different from those discussed in the other papers.

Keywords: *Incompressible couette flow, numerical method, partial differential equation, Crank--Nicolson implicit.*

1. Introduction

Couette flow is defined as follows. Consider the viscous flow between two parallel plates separated by the vertical distance H. The upper plate is moving at the velocity *u.;* and the lower plate is stationary; i.e., its velocity is $u = 0$. The flow in the *xy* plane is sketched in figure. The flow field between the two plates is driven exclusively by the shear stress exerted on the fluid by the moving upper plate, resulting in a velocity profile across the flow, $u = u(y)$, as sketched in figure.

The governing equation for this flow is the x-momentum equation.

$$\rho\frac{Du}{Dt}=\frac{\partial P}{\partial x}+\frac{\partial \tau_{xx}}{\partial x}+\frac{\partial \tau_{yx}}{\partial y}+\frac{\partial \tau_{zx}}{\partial z}+\rho f_x \qquad (1)$$

When applied to Couette flow, this equation is greatly simplified, as follows. from the continuity equation written for steady flow,

$$\frac{\partial(\rho u)}{\partial x}+\frac{\partial(\rho v)}{\partial y}=0 \qquad (2)$$

For all y, $v = 0$

Every where This is a physical characteristic of Couette flow, namely, that there is no vertical component of velocity anywhere. This states that the streamlines for Couette flow are straight, parallel streamlines-a result which is almost intuitively. We have, for Couette flow with no body forces,

$$0=-\frac{\partial \rho}{\partial y}+\frac{\partial \tau_{yy}}{\partial y} \qquad (3)$$

For Couette flow, there are no pressure gradients in either the *x* or *y* direction.

$$\tau_{xx}=\lambda\left[\frac{\partial u}{\partial x}+\frac{\partial v}{\partial y}\right]+2\mu\frac{\partial u}{\partial x}=0$$

$$\tau_{yx}=\lambda\left[\frac{\partial v}{\partial x}+\frac{\partial u}{\partial y}\right]+2\mu\frac{\partial u}{\partial x}=0$$

To substitute the above equation,

Fig 1: Schematic of Couette flow

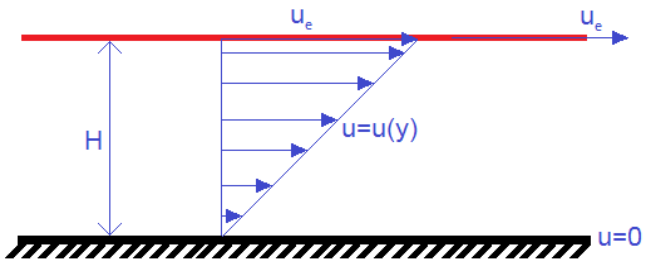

$$0=\frac{\partial}{\partial y}\left[\mu\frac{\partial u}{\partial y}\right]$$

At this stage, we will now assume an incompressible, constant-temperature flow for which $u =$ constant.

$$\frac{\partial^2 u}{\partial y^2}=0 \qquad (4)$$

The exact analytic solution of Eq.4 is straight forward. Integrating twice with respect to y, we have

International Journal of Scientific Engineering and Applied Science (IJSEAS) - Volume-1, Issue-4, June 2015
ISSN: 2395-3470
www.ijseas.com

$$u = c_1 y + c_2 \qquad (5)$$

where c1 and c2 are constants of integration; their values are found by applying the boundary conditions. Specifically, at the lower plate, we know that u=0 for y=0. From Eq.5, this yields c2=0. At the upper plate, we know that u=ue for y=H from Eq.5, this yields c1=ue/H. With these values for c1 and c2 Eq.5 becomes u/ue=y/H.

Equation u/ue=y/H is the exact, analytical solution for the velocity profile for incompressible Couette flow. Note from Equation u/ue=y/H that the exact result is a linear profile; u varies directly as y.

2.The NUMERICAL APPROACH:

IMPLICIT, Crank-Nicolson TECHNIQUE

We will pose the numerical solution as follows. Imagine that we assume a velocity profile which is not linear, i.e., a different velocity profile than the exact solution. Specifically, let us assume a velocity profile defined as

$$\begin{aligned} u &= 0 \qquad & 0 \le y < H \\ u &= u_e \qquad & y = H \end{aligned} \qquad (6)$$

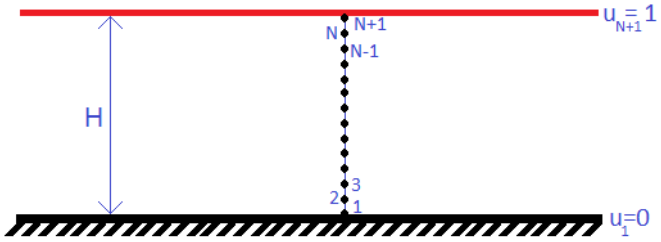

Fig 2: Labeling of points for the grid

The flow illustrated by the timewise-changing velocity profiles unsteady Couette flow. making the Couette flow assumptions of $\partial/\partial x = 0$ and $v = 0$ but carrying along the time derivative. The resulting governing equation, the *x*-momentum equation for unsteady, incompressible, Couette flow, is

$$\rho \frac{\partial u}{\partial t} = \mu \frac{\partial^2 u}{\partial y^2} \qquad (7)$$

Equation (7) is a parabolic partial differential equation; hence a time-marching solution represents a well-posed problem.

3.The Numerical Formulation

It will be convenient to deal with a nondimensional form of Eq. 7. Defining the following nondimensional variables

$$uu = \frac{u}{u_e} \qquad yy = \frac{y}{H} \qquad tt = \frac{t}{H/u_e}$$

Eq. 7 is nondimensionalized as follows.

$$\rho \frac{\partial (u/u_e)}{\partial (t/(H/u_e))} \left(\frac{u_e^2}{H} \right) = \mu \frac{\partial^2 (u/u_e)}{\partial (y/H)^2} \left(\frac{u_e}{H^2} \right)$$

$$\rho \frac{\partial uu}{\partial tt} = \frac{\mu}{\rho u_e H} \frac{\partial^2 uu}{\partial yy^2} \qquad (8)$$

$$\rho \frac{\partial uu}{\partial tt} = \frac{1}{\mathrm{Re}} \frac{\partial^2 uu}{\partial yy^2} \qquad (9)$$

Equation (9) is the equation for which we will obtain a numerical solution.

$$uu_j^{n+1} = uu_j^n + \frac{\Delta t}{2(\Delta y)^2 \,\mathrm{Re}} \times (uu_{j+1}^{n+1} + uu_{j+1}^n - 2uu_j^{n+1} - 2uu_j^n + uu_{j-1}^{n+1} + uu_{j-1}^n)$$

$$A = \frac{\Delta t}{2(\Delta y)^2 \,\mathrm{Re}} \qquad (10)$$

$$B = 1 + \frac{\Delta t}{(\Delta y)^2 \,\mathrm{Re}}$$

$$K_j = \left(1 - \frac{\Delta t}{(\Delta y)^2 \,\mathrm{Re}}\right) uu_j^n + \left(\frac{\Delta t}{(\Delta y)^2 \,\mathrm{Re}}\right)(uu_{j+1}^n + uu_{j-1}^n)$$

We choose to use an implicit finite-difference technique for this numerical solution; specifically, we will employ the Crank-Nicolson. In the present calculation, we will find that the incompressible

International Journal of Scientific Engineering and Applied Science (IJSEAS) - Volume-1, Issue-4, June 2015
ISSN: 2395-3470
www.ijseas.com

Couette flow solution illustrates all the pertinent features of an implicit solution using the Crank-Nicolson technique. It is important that you understand the basic ideas behind the Crank-Nicolson technique.

Following the Crank-Nicolson technique, the finite-difference representation of Eq. 9 is

Grouping all terms at time level n+1 in Eq.10 on the left-hand side and factoring both sides appropriately, Eq.10 becomes

$$Auu_{j-1}^{n+1} + Buu_{j}^{n+1} + Auu_{j+1}^{n+1} = K_j \qquad (11)$$

Equation 11 is solved on a grid such as that sketched in fig 2. The vertical distance (the *y* direction) across the duct is divided into N equal increments of length Δy by distributing N+1 grid points over the height H, that is,

$$\Delta y = \frac{H}{N}$$

From the boundary conditions, u_1 and u_{N+1} are known:

$$uu_1 = 0$$

$$uu_{n+1} = 1$$

With this, the system of equations represented by Eq.11 can be written, in matrix form, as

$$\begin{bmatrix} B & A & 0 & 0 & 0 & 0 & 0 & 0 & 0 \\ A & B & A & 0 & 0 & 0 & 0 & 0 & 0 \\ 0 & A & B & A & 0 & 0 & 0 & 0 & 0 \\ & & & & & & & & \\ & & & & & & & & \\ 0 & 0 & 0 & 0 & 0 & 0 & A & B & A \\ 0 & 0 & 0 & 0 & 0 & 0 & 0 & A & B \end{bmatrix} \begin{bmatrix} u_2^{n+1} \\ u_3^{n+1} \\ u_4^{n+1} \\ u_5^{n+1} \\ \\ \\ u_{N-1}^{n+1} \\ u_N^{n+1} \end{bmatrix} = \begin{bmatrix} K_2 \\ K_3 \\ K_4 \\ K_5 \\ \\ \\ K_{N-1} \\ K_N - Au_e \end{bmatrix}$$

Clearly, the system represented by Equation is in tridiagonal form. It can be solved using Thomas' algorithm.

3.The Setup

For our specific solution, we choose to use 21 grid points across the flow; i.e., in Fig.2, N+1=21. Since *y* is nondimensional, it varies from 0 to 1; hence

$$\Delta y = \frac{1}{20}$$

For initial conditions, we will use Eq.6 which yield

$$u_1, u_2, u_3, ..., u_{20} = 0 \quad at \quad t = 0$$

$$u_{21} = 0 \quad at \quad t = 0$$

The Crank-Nicolson technique is unconditionally stable; i.e., it is stable for all values of Δt. That is, stability considerations tell us that we can use as large a value of Δt as we wish. On the other hand, if we would want to simulate with any accuracy the actual transient variation of the flow field starting from the given initial conditions, we should keep Δt small in order to minimize the truncation error with respect to time. Of course, when we are interested in the steady state only, timewise accuracy is not a major concern.

$$\frac{1}{\mathrm{Re}} \frac{\alpha \Delta t}{\Delta y^2} \le \frac{1}{2}$$

$$\Delta t \le \frac{1}{2} \mathrm{Re} (\Delta y)^2$$

$$\Delta t = E\, \mathrm{Re} (\Delta y)^2 \qquad (12)$$

where *E* is a parameter. Since the Crank-Nicolson technique is unconditionally stable, we could choose *E* to be *any* value.

$$E = \frac{\Delta t}{\mathrm{Re} (\Delta y)^2}$$

Intermediate Results

Let us examine the calculation of the velocity profile for the first time step n=1. We choose E=1 and Re=1000. Also, since we are using 21 grid points across the flow, $\Delta y = 1/20 = 0.05$. With these values, we have for Δt from Eq. 12,

$$\Delta t = E\, \mathrm{Re} (\Delta y)^2 = 1 * 1000 * (0.05)^2 = 2.5$$

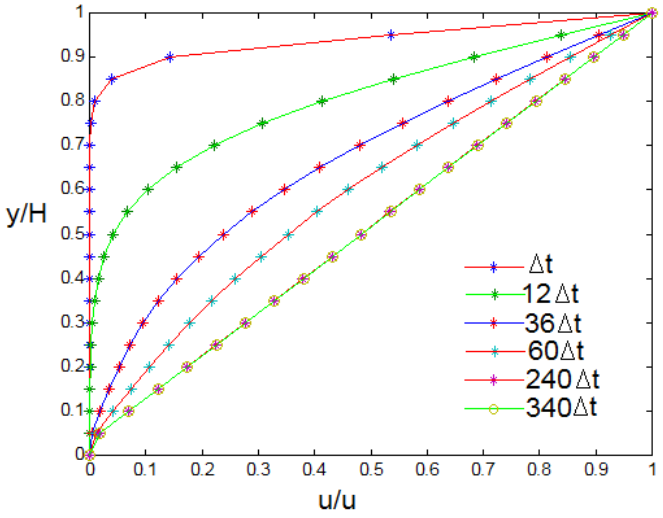

Fig 3: Velocity profiles for unsteady Couette flow at various stages in the time-stepping process

4.Final Results

The velocity profile after two time steps is labeled $t = \Delta t$ note that the velocity is changing most rapidly near the upper plate, as to be expected. Other profiles are shown in Fig.3 after 12, 36, 60, 240 and 340 time steps, The driving influence of the shear stress exerted by the upper plate is gradually communicated to the rest of the fluid, resulting in a final, steady-state profile after 200 time steps. This steadystate profile is linear, as to be expected; it agrees perfectly with the exact, analytical solution. To provide a more direct comparison of your computations with the present calculations.

All the above calculations were carried out with E = 1. *Question:* What is the effect of using a larger time step; i.e., reflecting on Eq. 12, what is the effect of using a larger value of E? In terms of stability, there should be no difference in the behavior of the solutions-the Crank-Nicolson technique is unconditionally stable. However, when E is increased, the accuracy of the transients may be compromised, and the number of marching steps required to obtain a steady state may change, for better or for worse. To address these matters, a numerical experiment is carried out wherein a number of different cases are calculated, each with a different value of E, with E ranging as high as 1000. From Eq. 12, we can interpret the effect of increasing E the same as increasing Δt for fixed Δy and Re. We will use this interpretation; whenever we refer to our increase in E, it will be synonymous with taking a larger time step, i.e., a larger Δt .

With this in mind, consider the velocity profiles tabulated in fig 4. And fig. 5. Three profiles are given, one each for E=5, E=10. These are transient profiles, all corresponding to the same nondimensional time t=300, this is an intermediate time-the steady-state profile corresponds to a

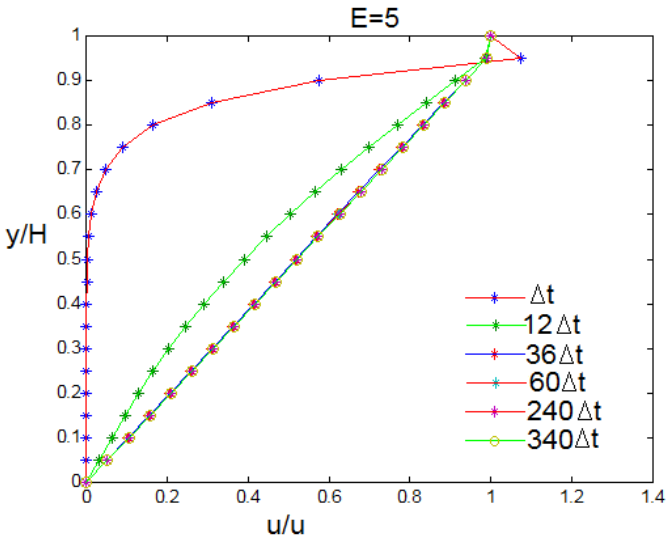

nondimensional time on the order of t=900.

Fig 4: Totally transient velocity profiles obtained when E=5

Of course, since different values of E eorrespond to different values of Δt then the three velocity profiles given in fig4 and fig 5, which correspond to the same value of t, tonsequently correspond to a different number of time steps. . We can feel comfortable that a value as high as E=1 provides timewise accuracy for the present implicit calculations. However, examine the last column in fig 4. For E=5. There are some differences between these results and those for E=1 especially near the upper wall (fig4 and fig 5.). Apparently E=10 corresponds to a large-enough

value of Δt to cause some noticeable inaccuracy for the transient results. This inaccuracy continues to grow as E>5 is further increased.

Fig 5: Totally transient velocity profiles obtained

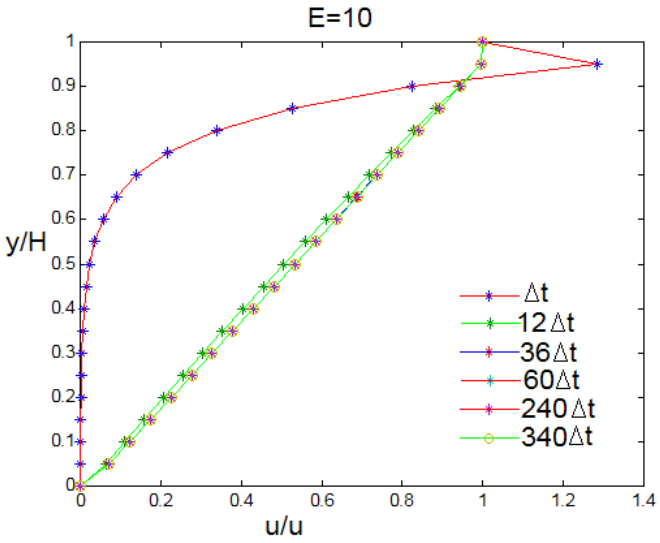

when E=10

Let us examine an extreme case, namely, one for E=1000. Here, the value of Δt is so large that no timewise accuracy can be expected, and none is obtained. Some results are plotted in Fig. 6. Six intermediate, transient velocity profiles are shown, one after one time steps and the other after 340 time steps; both profiles Δt and $12\Delta t$ exhibit totally nonphysical behavior, especially near the top plate. Compare these results in Fig. 6, obtained for E=1000, with the more realistic transient results shown in Fig. 3, obtained for E=1 there is no real comparison. The transient results in Fig. 6 are clearly nonphysical. However, after a very large number of time steps-on the order of 200-the implicit solution will finally converge to the proper steady-state velocity profile.

An aspect involving the number of marching time steps required to obtain the steady-state solution. For E=1, over 200 time steps are required to obtain the steady state; this is reflected in the results shown in fig. 3. For E=5, only about 36 steps are necessary to obtain the steady state, a tremendous savings in calculation time. For E=10, the steady state is obtained after 12 time steps, even better yet. However, for large values of E, the story reverses itself. And it gets worse as E is further increased.

Fig 6: Totally transient velocity profiles obtained

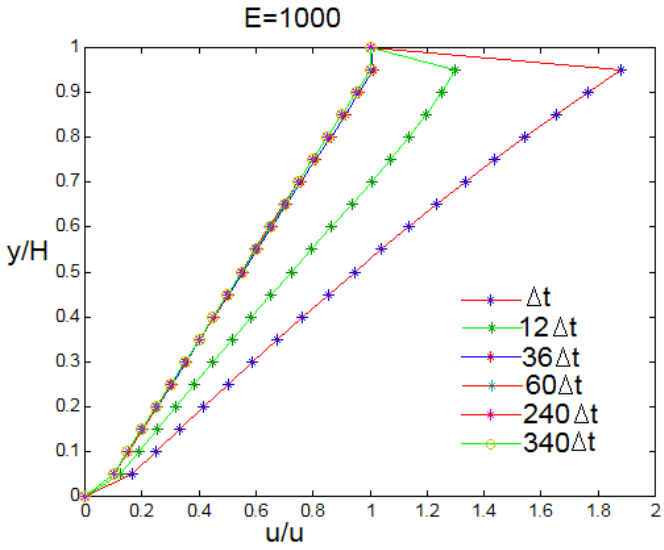

when E=1000

5.CONCLUSION

From the above numerical experiment associated with increasing the value of Δt (via increasing E), we can make the following conclusion regarding the behavior of the Crank-Nicolson implicit method as applied to the present problem:

By simply increasing the value of Δt (that is, increasing e), we first see a reduction in the number of time steps required to obtain a steady-state; this is consistent with the practical advantage of using an implicit method. However, for a large-enough value of in Δt (the present results, for E>5), the trend reverses itself, and as E increases further, more (not less) time steps are required to obtain the steady state. When we reach this condition, the practical value of using an implicit method is lost. In other words, there is some optimum value of E which leads to the most efficient implementation of the Crank-Nicolson method. For the present results, that optimum value of E is about 1(E=1).

REFERENCES

[1] Anderson, John D., Jr.: *Computational Fluid Dynamics*, The Basics Whit Applications, McGraw-Hill, New York, 1989.

[2] Anderson, John D., Jr.: *Hypersonic and High Temperature Gas Dynamics,* McGraw-Hili, New York, 1989.
[3] Rouse, Hunter, and Simon Ince: *History of Hydraulics,* Iowa Institute of Hydraulic Research, Ames, Iowa 1957.
[4] Tokaty, G. A.: *A History and Philosophy of Fluid Mechanics,* G. T. Foulis, Henly-on-Thames, England, 1971.
[5] Anderson, John D., Jr.: *The History of Aerodynamics, and Its Impact on Flying Machines,* Cambridge University Press, New York (in preparation).
[6] Kothari, A. P., and 1. D. Anderson, Jr.: "Flows Over Low Reynolds Number Airfoils-s-Compressible Navier-Srokes Numerical Solutions," AIAA paper 85-0107, presented at AIAA 23rd Aerospace Sciences Meeting, Reno, Nev., Jan. 14-17, 1985.
[7] Pohlen, L. 1., and T. 1. Mueller: "Boundary Layer Characteristics of the Miley Airfoil at Low Reynolds Numbers," *J Aircr.,* vol. 21, no. 9, pp. 658-664, September 1984.
[8] Anderson, John D., Jr.: *Fundamentals of Aerodynamics,* 2d ed., McGraw-Hili, New York, 1991.
[9] Bush, Richard J., Jr., Merle Jager, and Brad Bergman: "The Application of Computational Fluid Dynamics to Aircraft Design," AIAA paper 86-2651, 1986.
[10] Moretti, G., and M. Abbett: "A Time-Dependent Computational Method for Blunt Body Flows," *AIAA* **J,** vol. 4, no. 12, pp. 2136-2141, December 1966.
[11] Anderson, Dale A., John C. Tannehill, and Richard H. Pletcher: *Computational Fluid Mechanics and Heat Transfer,* McGraw-Hili, few York, 1984.
[12] Fletcher, C. A.: *Computational Techniques for Fluid Dynamics,* vol. I: *Fundamental and General Techniques,* Springer-Verlag, Berlin, 1988.
[13] Fletcher, C. A.: *Computational Techniques for Fluid Dynamics,* vol. II: *Specific Techniquesfor Different Flow Categories,* Springer-Verlag, Berlin, 1988.
[14] Hirsch, Charles: *Numerical Computation of internal and External Flows,* vol. 1: *Fundamentals of Numerical Discretization,* Wiley, New York, 1988.
[15] Hirsch, Charles: *Numerical Computation of Internal and External Flows,* vol, 11: *Computational Methods for lnviscid and Viscous Flows,* Wiley, New York, 1990.
[16] Hoffmann, K. A.: *Computational Fluid Dynamics for Engineers,* Engineering Education System, Austin, Tex., 1989.
[17] Hildebrand, Francis B.: *Advanced Calculus for Applications,* 2d ed., Prentice-Hall, Englewood Cliffs, N.J., 1976.
[18] Schlichting, H.: *Boundary Layer Theory,* 7th ed., McGraw-Hili, New York, 1979.
[19] Anderson, John D., Jr.: *Modern Compressible Flow: With Historical Perspective,* 2d ed., McGraw-Hill, New York, 1990.
[20] Kreyszig, *E.: Advanced Engineering Mathematics,* Wiley, New York, 1962.
[21] Whitham, G. 8.: *Linear and Nonlinear Waves,* Wiley, Iew York, 1974.
[22] Ames, W. F.: *Nonlinear Partial Differential Equations in Engineering,* Academic, New York, 1965.
[23] Courant, R., K. O. Friedrichs, and H. Lewy: "Uber die Differenzengleichungen der Mathematischen Physik," *Math. Ann,* voi. 100, p. 32, 1928.